ELSEVIER

Polymer Vol. 37 No. 12, pp. 2517–2524, 1996

0032-3861/96/$15.00 + 0.00

Growth and nucleation rate minima in long n-alkanes

S. J. Organ*, A. Keller† and M. Hikosaka‡
H. H. Wills Physics Laboratory, University of Bristol, Bristol BS8 1TL, UK

and G. Ungar†
Department of Engineering Materials, University of Sheffield, Sheffield S1 4DU, UK
(Received 26 March 1995)

The isothermal melt crystallization of the long pure n-alkanes, $C_{150}H_{302}$, $C_{198}H_{398}$, and $C_{246}H_{494}$, was studied by phase contrast and polarized optical microscopy. A custom-built T-jump cell was used. The crystal growth rates of $C_{150}H_{302}$, $C_{198}H_{398}$, and $C_{246}H_{494}$, and the rate of primary nucleation of $C_{246}H_{494}$ were measured directly. Both the growth and nucleation rates of crystals of $C_{246}H_{494}$ pass through a pronounced maximum and minimum with increasing supercooling. This unusual finding is in line with our previous observations of qualitatively the same behaviour of the overall crystallization rate of the alkanes $C_{246}H_{494}$ and $C_{198}H_{398}$ from both melt and solution. The rate minimum coincides with the transition between extended and once-folded chain crystallization. The slow down in nucleation and growth of extended-chain crystals is thought to be due to interference by frequent but unstable chain-folded depositions (surface 'self-poisoning'). Due to the high crystallization rates and experimental limitations, measurements could not be made at supercoolings which were sufficiently large to observe the minimum in $C_{150}H_{302}$ and $C_{198}H_{398}$, although an indication of the maximum is noticed in $C_{198}H_{398}$. In the vicinity of the extended-chain melting point the crystal growth rate G increases linearly with the increasing supercooling ΔT. The dependence of the slope on the molecular length l could be approximated by $dG/d(\Delta T) \propto l^{-8.5}$ for the three alkanes studied here. The morphological features, as well as the differences between growth and nucleation kinetics, are discussed. Copyright © 1996 Elsevier Science Ltd.

(Keywords: polymer crystallization; normal alkanes; surface poisoning)

INTRODUCTION

The high-purity long n-alkanes synthesized by Whiting and coworkers[1,2] provide invaluable model materials for studying the onset of chain folding. The materials available cover a range of chain lengths which on crystallization give rise to crystals containing chains which may be extended or folded up to four times[3]. Among significant results documented in detail elsewhere it has been shown that stable crystal forms have thicknesses equal to exact integer fractions (IFs) of the extended chain length[4,5]. Non-integer fraction (NIF) crystal thicknesses may occur during the early stages of crystallization but subsequently transform via isothermal thickening or thinning to IF values[6].

Crystallization rates have been measured on melt-crystallized $C_{246}H_{494}$ by differential scanning calorimetry (d.s.c.) and time-resolved synchrotron X-ray experiments[7] and on $C_{198}H_{398}$, crystallized from both melt and solution, by d.s.c.[7,8]. All three systems have revealed the presence of a pronounced minimum in crystallization rate at temperatures in the region where folded-chain crystals are first obtained. This minimum in crystallization rate has been attributed to a 'self-poisoning' effect, whereby the growth front of potentially stable extended-chain crystals is repeatedly blocked by the deposition of transient folded-chain conformations[9]. The concept of 'self-poisoning' is further reinforced by d.s.c. and morphological studies of isothermal thickening in solution-grown once-folded chain crystals of $C_{198}H_{398}$[10,11]. A shallow crystallization rate minimum has also been reported in a low-molecular-weight fraction of methoxy-capped poly(ethylene oxide) by Cheng and Chen[12], following the classic earlier work on such systems by Kovacs *et al.*[13,14]. In their recent work on alkanes of similar chain lengths to ours, but prepared by a different synthetic route[15], Mandelkern and coworkers[16] do not find evidence for crystallization-rate minima. While we can only speculate as to the reasons for this, a careful reading of our original reports[7,8] will suffice to alleviate any doubts expressed in ref. 16 regarding the authenticity of the rate minima in pure alkanes. This present work provides further evidence for rate minima, obtained by yet another experimental technique.

In all of the studies mentioned so far it has been impossible to separate the individual influences of nucleation and growth on the overall crystallization rate and hence to determine the precise origin of the minimum. In this paper we present results obtained from direct

* Present address: Weston College, Knightstone Road, Weston-super-Mare, BS23 2AL, UK
† To whom correspondence should be addressed
‡ Present address: Faculty of Integrated Arts and Sciences, University of Hiroshima, Higashi-Hiroshima 724, Japan

observation of crystal growth in thin films of $C_{150}H_{302}$, $C_{198}H_{398}$, and $C_{246}H_{494}$, made possible by the construction of a specially designed hot-stage allowing instantaneous change of temperature from above the melting point (T_m) to a crystallization temperature T_c. Linear growth rates have been measured in $C_{150}H_{302}$, $C_{198}H_{398}$, and $C_{246}H_{494}$, and nucleation rates in $C_{246}H_{494}$. A pronounced minimum is observed in both growth and nucleation rate for $C_{246}H_{494}$, with the effect being slightly more pronounced in the nucleation rate measurements. Crystal morphologies are unfortunately not well resolved, but some general comments may be made.

EXPERIMENTAL

Small samples of $C_{150}H_{302}$, $C_{198}H_{398}$, and $C_{246}H_{494}$, were melted and pressed between microscope cover slips to give thin films of approximately 25 μm in thickness. These samples were then inserted into a specially designed 'T-jump' microscope hot-stage, as illustrated in *Figure 1*. The temperature of the hot-stage is measured at two positions, A and B, with the temperature at each position independently set and maintained using Eurotherm temperature controllers with an accuracy of ± 1°C at A and ± 0.1°C at B. Position A is generally used for melting the sample and is therefore set to be slightly higher than the melting point of the n-alkane in use, namely ~ 128°C for $C_{198}H_{398}$ and ~ 130°C for $C_{246}H_{494}$. Position B is set to the crystallization temperature. The sample may be rapidly moved from A to B by means of the sliding sample frame and thus reaches the required T_c in the minimum possible time. A window in the hot-stage allows the sample to be viewed at B. The hot-stage was attached to a Zeiss Ultraphot optical microscope set up for phase contrast, and the isothermal crystallization was recorded at a series of different temperatures by using a U-matic video system incorporating timing and measuring devices. Growth and nucleation rates were subsequently measured directly from the video screen—growth rates by choosing isolated well-defined crystals and measuring their dimensions at regular intervals during crystallization, and nucleation rates by counting the number of crystals growing within a defined area as a function of crystallization time. Measurements of crystal size were always taken along the longest crystal dimension where this could be ascertained.

Crystal morphologies in $C_{150}H_{302}$ and $C_{198}H_{398}$ were well defined, since low nucleation densities generally permitted crystals to grow to several micrometres in size before impinging upon each other. At the higher crystallization temperatures morphologies could be 'quenched-in' by using the self-decoration technique developed by Kovacs and Gonthier[17]. Samples for quenching, pressed into thin films between cover slips as described previously, were crystallized separately in oil baths. After the required crystallization time (t_c) the cover slips were removed and rapidly transferred into a mixture of dry ice and acetone, causing instantaneous rapid nucleation around the periphery of the crystal and within the surrounding melt. This technique was not successful in $C_{246}H_{494}$ where, at all but the highest T_cs, the small size of the crystals led to their outlines being obliterated by overgrowth on quenching.

RESULTS

$C_{150}H_{302}$

In *Figure 2* we show crystal growth rate data (G) for the alkane $C_{150}H_{302}$. As can be seen, the growth rate increases steeply with decreasing crystallization temperature and, as a result, only a narrow temperature range could be investigated. Each experimental point in *Figure 2* is an average of several measurements. Because of the steep gradient, dG/dT_c, the accuracy in G is lower than in other experiments. No indication of a maximum

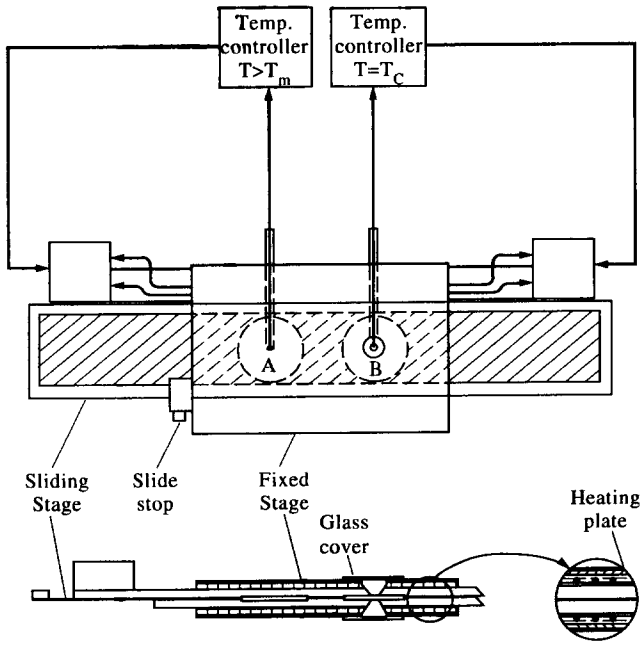

Figure 1 Top and side views of the T-jump microscopy stage used in this work. The specimen is mounted on a slide which allows it to be transferred rapidly from position A on the left to B, which contains a viewing aperture, on the right; A is set at $T > T_m$ and B at $T_c < T_m$

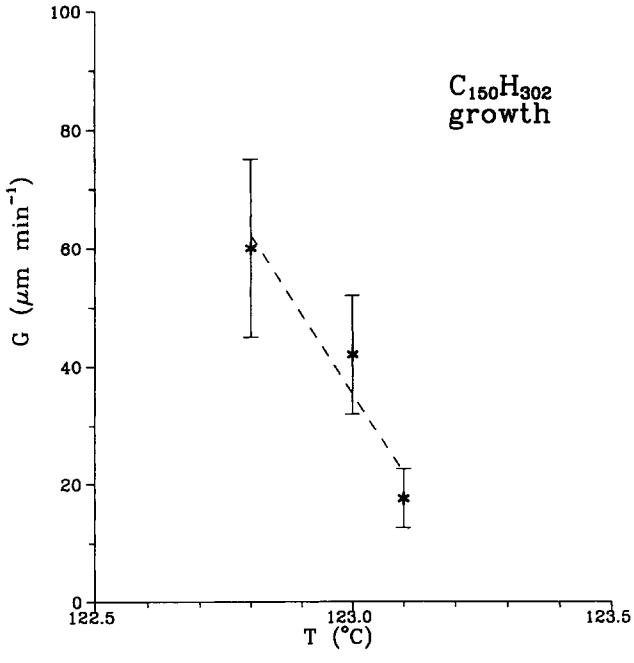

Figure 2 Linear growth rate (G) of crystals of $C_{150}H_{302}$ as a function of crystallization temperature T_c; the line of best fit is shown

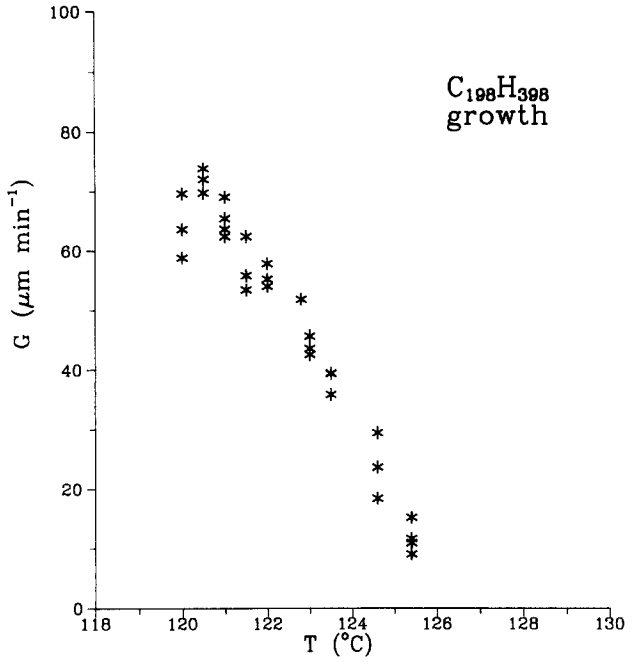

Figure 3 Linear growth rates (G) of crystals of $C_{198}H_{398}$ as a function of crystallization temperature T_c

or minimum in G is evident, nor is it expected at this small supercooling.

$C_{198}H_{398}$

Figure 3 shows the linear growth rates (G) of crystals of $C_{198}H_{398}$ as a function of crystallization temperature. Each point represents the result from an individual crystal. The crystals chosen for measurement were generally the largest in view and were assumed to be lying flat. Although some tilt would be possible within the film thickness used, the regularity in crystal shape throughout the sample suggested that any effect of tilt was small. The results in *Figure 3* show a linear increase in growth rate as T_c is lowered, with a small reduction in growth rate at $T_c = 120.5°C$. Some representative crystal morphologies are shown in *Figure 4*. The outlines of the crystals have been delineated using the self-decoration technique described above, and the crystals are imaged between crossed polars. The high birefringence contrast seen in the photographs developed on quenching; during the isothermal crystallization the crystals were only very weakly birefringent. At the highest T_c values crystals typically begin growing as isolated leaf-shaped lamellae, and an example of this can be seen in the left-hand side of *Figure 4a*. As crystallization proceeds several crystals begin to grow from a common nucleation site, as shown in *Figure 4b* and, to a larger extent, in the right-hand side of *Figure 4a*. This trend towards multiple nucleation increases greatly as T_c is reduced, thus producing a spherulitic-type morphology, as shown in *Figure 4c*. Spherulites, sometimes banded, can also be seen throughout the quenched background material. Similar morphologies occurred over the whole T_c range studied, although increasing nucleation densities limited the size of crystals grown at lower temperatures.

$C_{246}H_{494}$

Figure 5 shows the variation in linear growth rate (G) with crystallization temperature for $C_{246}H_{494}$. Each point represents an individual measurement, as before. As the supercooling is increased, an initial rise in growth rate is observed, as expected. However, on increasing the supercooling further the growth rate passes through a maximum at $T_c = 123.0°C$, subsequently falling to a minimum value at $T_c = 120.0°C$. As the crystallization

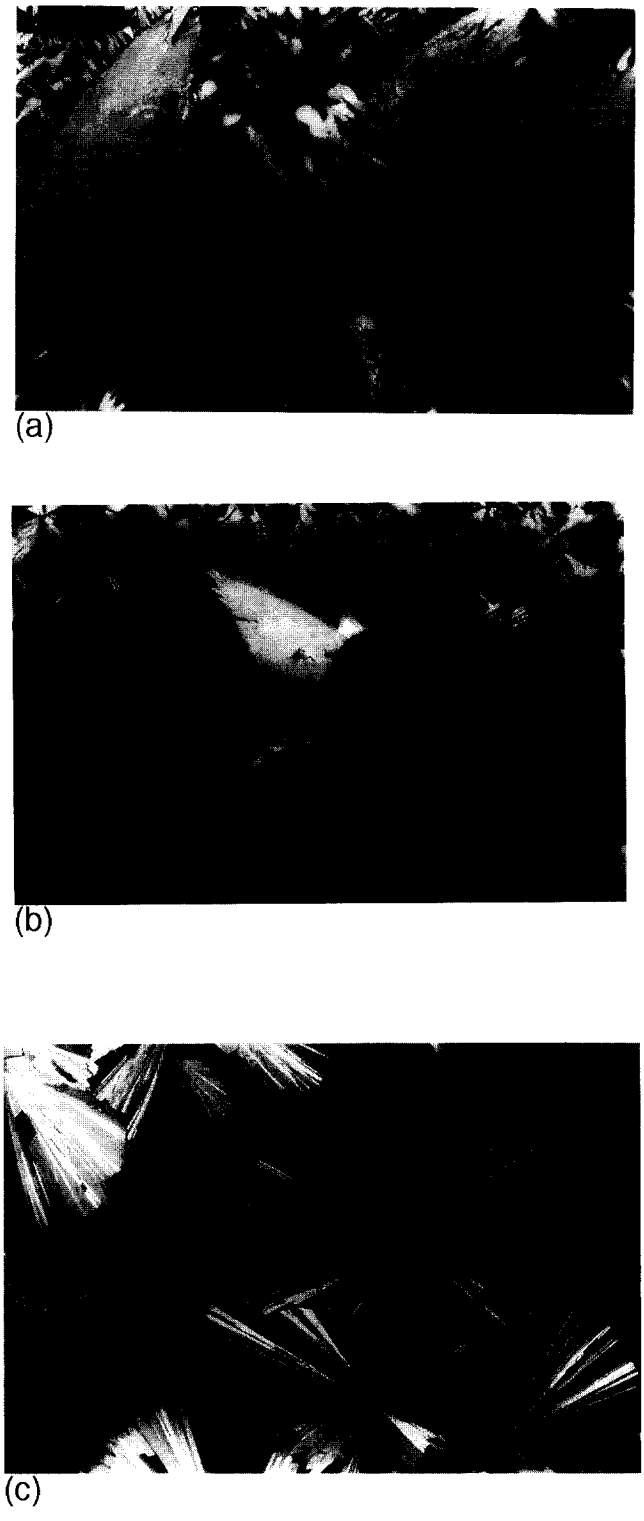

Figure 4 Optical micrographs of $C_{198}H_{398}$ taken with crossed polarizers; the samples were crystallized isothermally from the melt at $T_c = 124.3°C$ (a and b) and 122.0°C (c), and subsequently quenched (the self-decoration technique[17]). The full width (horizontal) of the photographs corresponds to (a) 0.9, (b) 1.1 and (c) 1.3 mm

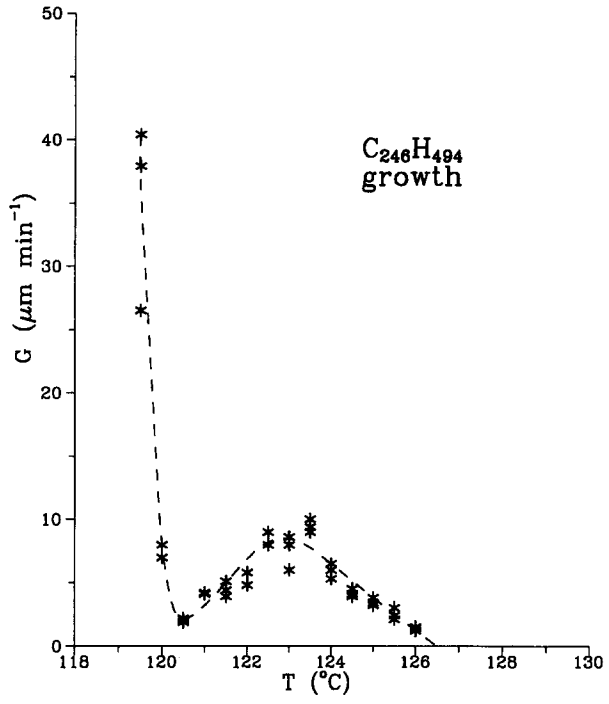

Figure 5 Linear growth rate (G) of crystals of $C_{246}H_{494}$ as a function of crystallization temperature T_c

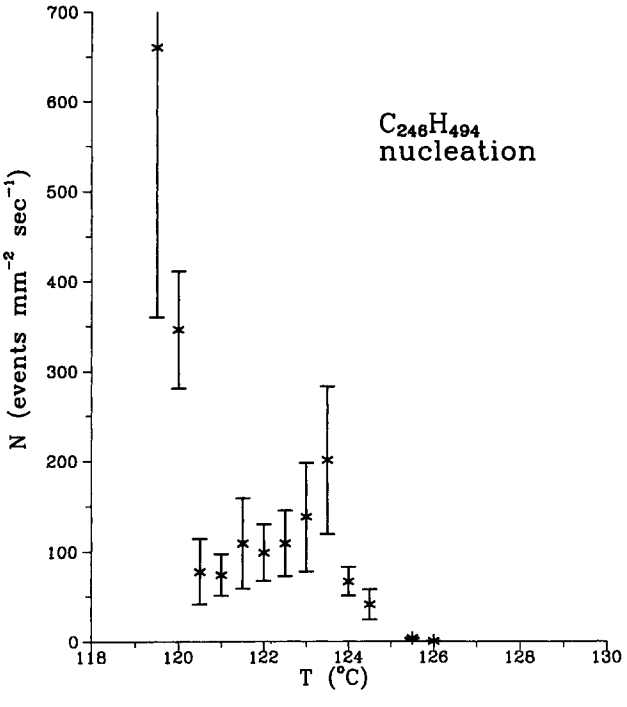

Figure 6 Nucleation rates (i) for $C_{246}H_{494}$ as a function of crystallization temperature T_c; nucleation rates are quoted in events mm^{-2} s^{-1}

temperature is reduced further the growth rate very quickly begins to rise once more, soon becoming too fast to measure by using our apparatus.

Nucleation rates (i) were also measured over the same range of temperatures and these results are shown in *Figure 6*. Nucleation rates are quoted in events mm^{-2} s^{-1}. Absolute values could not be obtained as the thickness of the film was not known precisely. However, since the same sample was used in each case, the results are directly comparable with each other. The bars on the graph represent one standard deviation from several (typically ~10) measurements. The nucleation rates vary with crystallization temperature in a very similar manner to the growth rates. At low supercoolings, the nucleation rates also increase with supercooling until reaching a maximum at 123.5°C. As the supercooling is reduced further the nucleation rates decrease, passing through a minimum value at T_c = 121.0°C, then rising steeply for T_c < 120.5°C.

Corresponding crystal morphologies of $C_{246}H_{494}$ were well defined only at the highest growth temperatures. *Figure 7* shows examples of crystals obtained at 126.5°C (*Figure 7a*) and 125.5°C (*Figure 7c*): the crystals are imaged in phase contrast and prints have been taken from the video recording. The crystal shapes can be more clearly seen in *Figures 7b* and *7d*, where their outlines have been drawn from the photographs. In this region, the morphology is clearly leaf-shaped, similar to that seen in $C_{198}H_{398}$ but with a much reduced tendency towards multiple nucleation. As the temperature is reduced further towards the maximum in G and i, elongated crystal shapes persist but their size is limited by the greater nucleation densities. As the temperature is reduced further the crystals become more 'blobby' in character, although the precise shapes are impossible to determine. *Figure 8* shows examples of crystals grown at temperatures in the region of the minima in growth and nucleation rates, at 120.0 (*Figure 8a*) and 121.0°C (*Figures 8c* and *8e*), respectively: the crystal outlines have been drawn alongside (*Figures 8b*, *8d* and *8f*). At temperatures in the region between the minima and maxima in growth and nucleation rates a very characteristic

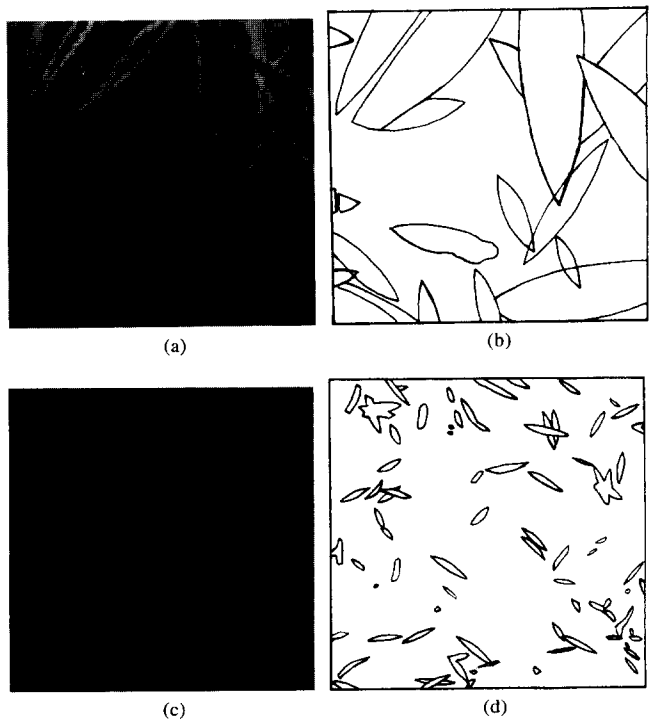

Figure 7 Photomicrographs (phase contrast) of $C_{246}H_{494}$ recorded during crystallization at 126.0°C and t_c = 20 min (a) and 125.0°C and t_c = 10 min (c); for clarity, crystal outlines of (a) and (c) are drawn, respectively, in (b) and (d). The width of the pictures corresponds to (a, b) 0.12 and (c, d) 0.20 mm

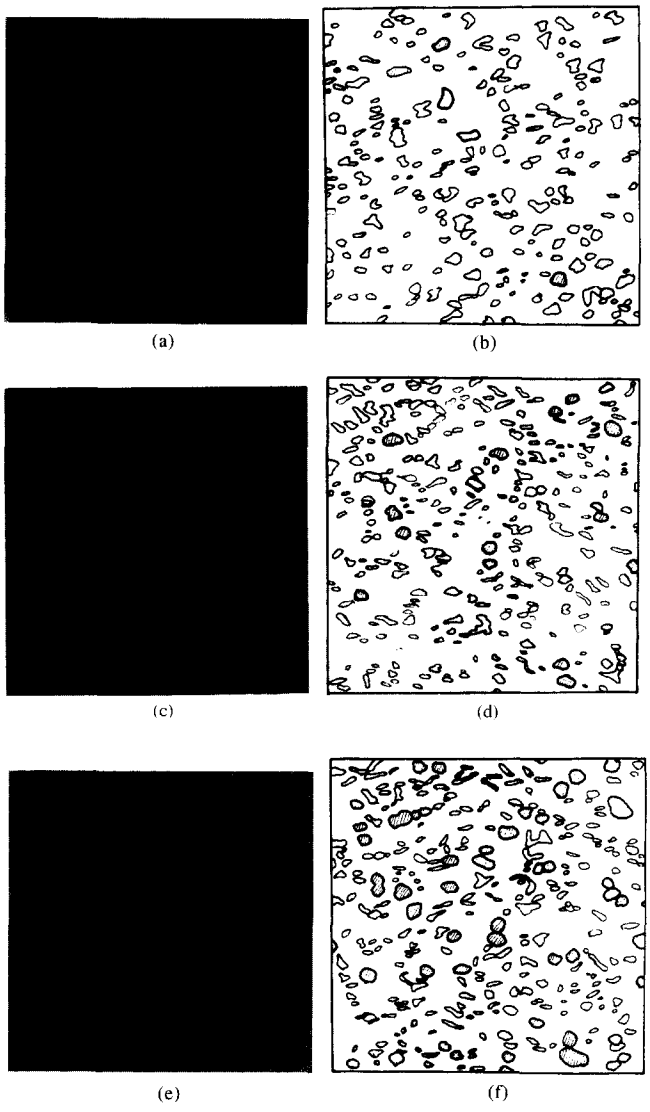

Figure 8 Photomicrographs (phase contrast) of $C_{246}H_{494}$ recorded during crystallization at around the temperature of the rate minimum: (a) and (b) $T_c = 120.0°C$, $t_c = 6$ min; (c) and (d) $T_c = 121.0°C$, $t_c = 4$ min; (e) and (f) $T_c = 121.0°C$, $t_c = 5$ min. The width of all pictures corresponds to 0.2 mm

thickening behaviour is seen, and this is illustrated in *Figures 8c–f*. Crystals begin growing as thin lamellae, visible in phase contrast as faint grey patches. As crystallization proceeds, some of these crystals become very much thicker and start to glow brightly in phase contrast. The thickened crystals continue to grow and increase in number as crystallization proceeds. This process can be seen in *Figure 8*, where a few thickened crystals are visible as lighter patches ringed with black in *Figure 8c*, with these being shaded in *Figure 8d*. After growing for a further minute there are many more of these bright patches visible, as can be seen in *Figures 8e* and *8f*. Such behaviour was only observed in the temperature range between the minima and maxima in growth and nucleation rates.

DISCUSSION

The general shape of the growth and nucleation rate curves as functions of the supercooling will be discussed first, with special reference to the observed maximum and minimum. This will be followed by a consideration of rates close to the extended-chain melting point, i.e. above the temperature of the rate maximum. Extended-chain-crystal growth rates will then be compared for alkanes of different length. The rates of primary nucleation at small supercoolings will then be contrasted to those of crystal growth. Finally, a brief discussion of crystal morphologies will be presented.

The rate minimum

Figures 5 and *6* clearly show the presence of a maximum and a minimum in the rates of both crystal growth and primary nucleation as a function of the supercooling ΔT. This result confirms and extends our earlier reports[7,8] of maxima and minima in the overall crystallization rate of the n-alkanes $C_{246}H_{494}$ and $C_{198}H_{398}$. While previous measurements of overall crystallization rates could not distinguish between the contributions of growth and nucleation, it was evident from non-isothermal experiments that the anomaly was present at least in the crystal-growth rate, if not in both the growth and the nucleation (see below). The value of the current results is in the finding that both the rates of growth and nucleation display the anomaly, and also in providing quantitative data on the temperature dependence of the two rates, separately.

In the case of $C_{246}H_{494}$ and with the present T-jump microscopy cell we were able to measure both the growth and nucleation rates over the full range of extended-chain crystallization, as well as at the very top end of the once-folded temperature range. Unfortunately, the same cannot be said for $C_{198}H_{398}$ and even less for $C_{150}H_{302}$. The reason that only the upper part of the extended-chain temperature range could be investigated quantitatively for shorter n-alkanes is twofold: as the chains become shorter, (a) the crystal growth rate increases more steeply with increasing ΔT (see next section), and (b) the temperature range of extended-chain crystallization widens, thus increasing the relative supercooling at which the rate minimum occurs.

The latter point is illustrated in *Table 1*, which lists the d.s.c. melting temperatures relevant to the present discussion, where T_m^E and T_m^F are the melting points of the extended and once-folded chain forms, respectively. It should be mentioned that T_m^F cannot be measured in these alkanes with the same accuracy as T_m^E since, first, chain-folded crystals are metastable and recrystallize during melting and, secondly, they cannot be annealed close to their melting point.

Considering $C_{198}H_{398}$, although the growth rate increases monotonically with increasing supercooling for the greater part of the measured range (*Figure 3*), it is significant that a small decrease in rate is recorded

Table 1 D.s.c. melting temperatures of extended (T_m^E) and once-folded (T_m^F) chain crystals of n-alkanes $C_{246}H_{494}$, $C_{198}H_{398}$ and $C_{150}H_{302}$

n-Alkane	T_m^E (°C)	T_m^F (°C)	$T_m^E - T_m^F$ (°C)
$C_{246}H_{494}$	128.(6)	123	5.(6)
$C_{198}H_{398}$	126.(4)	118	8.(4)
$C_{150}H_{302}$	123.(5)	–	–

at the lowest temperature of 120.5°C. This decrease has been confirmed by several separate experiments. Unfortunately, repeated attempts to measure growth rate at still larger ΔT values, failed due to a strongly enhanced primary nucleation rate which, unlike the growth rate, tends to increase exponentially with supercooling. While, admittedly, the growth rate maximum at 121°C requires further confirmation, its position is in the expected range, i.e. in the lower half of the temperature range between T_m^E and T_m^F. It should, of course, be borne in mind that $C_{198}H_{398}$ shows a very pronounced minimum in the crystallization rate from solution[8].

In spite of experimental difficulties in determining the isothermal growth rates in the complete temperature range of extended-chain crystallization, the existence of the growth rate maximum and minimum in the melt crystallization of $C_{198}H_{398}$ has been proven beyond doubt by a non-isothermal experiment[7]. On cooling this alkane at a rate of 40°C min^{-1} two clearly separated d.s.c. exotherms are observed, i.e. a smaller one at 122°C and a larger one at 120°C. The two are separated by a minimum in heat outflow, thus indicating a minimum in the rate of crystallization, in spite of the bulk of the sample still being molten at that point. Thus, even if nucleation ceased completely, the growth of existing crystals would have continued at an increased rate, had it not been for the minimum in the rate of crystal growth. The same behaviour, resulting in a d.s.c. thermogram with a double exotherm of an almost identical shape, has been observed for $C_{246}H_{494}$ at a lower cooling rate of 1°C min^{-1}.

In contrast to $C_{198}H_{398}$, the considerably lower crystallization rate, combined with a narrower temperature range between T_m^E and T_m^F, meant that for $C_{246}H_{494}$ both the rates of crystal growth and primary nucleation could be measured in the entire extended-chain range. Thus the resulting growth and nucleation rate data, plotted in *Figures 5* and *6* as functions of the supercooling, show the maximum and the minimum in their entirety. In the case of crystal growth, for which the rate increases linearly with supercooling at small ΔT values (see further below), the extrapolated 'zero growth' temperatures $T_m^{E'}$ and $T_m^{F'}$ for the two rate branches differ by ca. 6°C, in line with the difference $T_m^E - T_m^F$ (*Table 1*). This close agreement in itself suggests that the sharp upturn in crystallization rate below the temperature of the minimum coincides with the onset of once-folded crystallization. This has in fact already been confirmed by a direct time-resolved synchrotron small-angle X-ray scattering (SAXS) experiment[7].

A qualitative explanation of the anomalous temperature dependence of the crystal growth rate has been proposed in a previous publication[9]. It was postulated that at temperatures slightly above $T_m^{F'}$, transient, almost-stable chain-folded depositions form frequently and block the advance of the extended-chain growth front. Thus, as $T_m^{F'}$ is approached from above, the extended-chain growth rate decreases in spite of an increasing driving force for crystallization. This effect was termed 'self-poisoning', because the model implies that the crystal surface is poisoned not by impurities but by native molecules in a 'wrong', i.e. folded, conformation. Regarding the retardation of the process of primary nucleation (*Figure 6*), it is likely that a qualitatively similar mechanism as the one just described is responsible also in the formation of the critical nucleus.

Simultaneously, but independently of the first discovery of the crystallization rate minimum, Sadler and Gilmer[18] obtained the growth-rate minima theoretically when applying their two-dimensional row model of stems to a system with several preferred stem lengths. In a recent study by Higgs and Ungar[19] both the rate equation approach using the row model and a quasi-3-dimensional simulation accurately reproduced the observed shape of the growth-rate maximum and minimum observed in the alkane $C_{246}H_{494}$. The model was simple, with a stem consisting of either one (chain-folded) or two (chain-extended) crystallizing segments. As in ref. 18 the essential condition for growth to proceed was that all of the folded overlay be removed at the particular location to allow a chain at the crystal surface to extend. In the case of the rate minimum, the hindrance to growth, i.e. self-poisoning, is the extreme manifestation of Sadler's kinetic 'entropy barrier', considered to be dominant in polymer crystal growth.

In fact, the crystal-growth rate obtained by the above calculation, as well as by the Monte Carlo simulation, went to zero at the minimum, as the width of the chain-folded overgrowth diverged[19]. In order to maintain a finite rate at the minimum, an additional slow process of chain extension by solid-sate diffusion had to be invoked, whereby folded stems adjacent to extended ones do not always need to detach and re-attach for a change of conformation to occur. It was suggested that this solid-state process, being reasonably fast at the temperatures of melt crystallization but almost absent at the lower temperatures of crystallization from solution, accounts for the observation that the minimum in melt crystallization is much shallower than that in crystallization from solution, where growth ceases almost completely[8].

An alternative explanation of the rate anomaly has been proposed by Hoffman[20] in terms of the secondary nucleation theory. A comment by one of us on this alternative explanation has already been published elsewhere[21].

Crystal growth at small supercoolings

We are now turning to the growth rates of extended-chain crystals at low supercoolings, well away from the temperature region of the rate minimum. It is clear from *Figures 3*, *5*, and *2* that G increases linearly with the supercooling ΔT for all alkanes close to their extended-chain melting temperature. The linear dependence of G on ΔT has also been observed previously for poly(ethylene oxide) (PEO) fractions[12,14,22], as well as for the n-alkane $C_{94}H_{190}$[23] and for a sharp low-molecular-weight polyethylene fraction[24]. Point and Kovacs[25] have argued that this linear dependence contradicts the Lauritzen–Hoffman (LH) nucleation theory of polymer crystallization, which, in its earlier version, would have predicted an exponential dependence. However, a linear dependence of the growth rate on the undercooling ΔT, as follows:

$$G \simeq K\Delta T \qquad (1)$$

is derived in later versions of the LH theory for crystals with fixed l values[26]. As with other applications of the LH theory, the value of the constant K is regime-dependent. The linear dependence of the crystal growth

Table 2 Initial linear slope of crystal growth rate vs. supercooling

Alkane	$K = dG/dT_c$ ($cm\ s^{-1}\ K^{-1}$)
$C_{150}H_{302}$	2.4×10^{-4}
$C_{198}H_{398}$	2.6×10^{-5}
$C_{246}H_{494}$	4.5×10^{-6}

rate on ΔT follows naturally also from the rough-surface growth theory of Sadler for lamellae of constant l[22,27,28].

It should be remarked that in real experimental systems the linear-growth-rate dependence can only be expected to hold all the way to the zero-growth temperature for absolutely monodisperse chains. For polymer fractions there is always a curvature in $G(\Delta T)$, near the zero-growth temperature, which is associated with fractionation[14,21,22].

The values of the gradient K of growth rate vs. temperature (equation (1)), as determined from *Figures 2*, *3*, and *5*, are given in *Table 2* for different alkanes. K is clearly very sensitive to chain length. There is an order-of-magnitude difference in K between each of the three successive alkanes $C_{150}H_{302}$, $C_{198}H_{398}$, and $C_{246}H_{494}$. The chain length dependence of K can be represented by the following:

$$K \propto l^{-n} \tag{2}$$

where $n = 8.5$ (± 1.5). A similar analysis of the growth-rate data for PEO fractions gave an l^{-7} dependence of K[22]. Given the experimental error and some difference in the range of the l values between the two sets of data, we do not wish to emphasize the difference in the value of the exponent obtained from n-alkanes and PEO. The implications of the K vs. l dependence for the crystallization theory are presently being considered.

Crystal morphology

The extended-chain crystals of $C_{198}H_{398}$ (*Figures 4a* and *4b*) and $C_{246}H_{494}$ (*Figure 7*) grown at low supercooling are leaf shaped, or lenticular, with curved edges and more or less pointed ends. Such morphology is typically observed in polyethylene single crystals grown at high temperatures[29,30] and has also been observed in melt-crystallized polyethylene[31,32]. The long axis in such crystals is the b-axis. The current understanding is that this morphology is caused by the (110) faces advancing considerably faster than the (100) faces during crystal growth, with the curvature of the latter resulting from retarded step propagation[33]. The occurrence of pointed crystal tips, as observed in the above figures, has been specifically attributed to the rate of step propagation ν being smaller than the (100) substrate spreading rate h; in other words, the steps lag behind the corners[30]. An alternative interpretation of rounded crystal habits is based on reflecting boundary conditions in the Frank equation for step propagation[34,35].

The reason for the slow substrate completion rate leading to curved crystal faces is unknown and self-poisoning has been suggested as a possibility for this occurrence[30]. In PEO fractions, where re-examination of the original growth rate data of Kovacs *et al.*[14] revealed an anomalous retardation near the extended-to-folded growth transition[21], the retardation is accompanied by a change in crystal habit[12,22]. Below, and also well above the transition temperature, the crystals have facets, which show slight curvature. However, at and just above the transition, where self-poisoning appears to be pronounced, the crystals are circular. Unfortunately, for reasons given in the Results section of this present paper, we have not succeeded in obtaining good quality micrographs of $C_{246}H_{494}$ crystals near the rate minimum. Nevertheless, it is clear from *Figures 8c–f* that many of the small 'blobs' which appear bright in phase contrast near the temperature of the minimum are circular or close to circular in shape, and are distinctly less anisometric than the elongated crystals which are observed at higher temperatures.

It can thus be said that the present limited morphological evidence supports the trend that was previously established for PEO fractions for self-poisoning to be associated with circular crystal habits[21]. If it is true that retarded step propagation, leading to curved crystal faces, is caused by self poisoning, then it is not difficult to extrapolate to the situation envisaged in the vicinity of the growth-rate minimum where surface obstruction to growth become exceptionally prominent. In the extreme case, step propagation is virtually halted and growth ceases to be a nucleation-controlled process, leading to a high degree of surface roughness. A very high degree of kinetic surface roughening has indeed been observed in the simulation of the growth of alkane crystals near the growth rate minimum[19].

We wish to point to the fundamental difference between the present kinetic roughening caused by self-poisoning and the equilibrium surface roughening, invoked by Sadler in his roughness-pinning theory of crystal growth[36]. However, both types of roughening can lead to curved-faced, ultimately circular, crystals.

CONCLUSIONS

It is shown by direct measurement using optical microscopy that both the linear growth rate and primary nucleation rate of crystals of the n-alkane $C_{246}H_{494}$ pass through a pronounced maximum and minimum with increasing supercooling. These findings further confirm and compound our previous observations of similar effects in the overall crystallization rate from both melt and solution of the alkanes $C_{246}H_{494}$ and $C_{198}H_{398}$; previously, however, the growth and nucleation rates could not be separated.

Furthermore, we find that in the vicinity of the extended-chain melting point the crystal growth rate G increases linearly with increasing supercooling ΔT, in line with both the nucleation (LH) theory and the roughness-pinning theory of polymer crystallization constrained to a fixed lamellar thickness. The chain length (l) dependence of the slope is found to be of the form $dG/d(\Delta T) \propto l^{-8.5}$ for alkanes in the range $C_{150}H_{302}$–$C_{246}H_{494}$.

The extended-chain crystals grown at small ΔT are leaf shaped, and apparently become progressively more circular as the growth-rate minimum is approached. The results support the self-poisoning hypothesis, according to which almost stable chain-folded depositions obstruct the productive process of extended-chain-crystal growth. For the first time, this effect is shown to also act in retarding primary crystal nucleation.

ACKNOWLEDGEMENT

The authors are indebted to Professor A. Kovacs for introducing SJO to the technique of self-decoration of melt-grown crystals.

REFERENCES

1 Bidd, I. and Whiting, M. C. *J. Chem. Soc. Chem. Commun.* 1985, 543
2 Bidd, I., Holdup, D. W. and Whiting, M. C. *J. Chem. Soc. Perkin Trans. 1* 1987, 2455
3 Ungar, G., Stejny, J., Keller, A., Bidd, I. and Whiting, M. C. *Science* 1985, **229**, 386
4 Organ, S. J. and Keller, A. *J. Polym. Sci. Polym. Phys. Edn* 1987, **25**, 2409
5 Ungar, G., Organ, S. J. and Keller, A. *J. Polym. Sci. Polym. Lett. Edn* 1988, **26**, 259
6 Ungar, G. and Keller, A. *Polymer* 1986, **27**, 1835
7 Ungar, G. and Keller, A. *Polymer* 1987, **28**, 1899
8 Organ, S. J., Ungar, G. and Keller, A. *Macromolecules* 1989, **22**, 1995
9 Ungar, G. in 'Integration of Fundamental Polymer Science and Technology' (Eds P. J. Lemstra and I. A. Kleintjens), Vol. 2, Elsevier, London, 1988, p. 346
10 Organ, S. J., Ungar, G. and Keller, A. *J. Polym. Sci. Polym. Phys. Edn* 1990, **28**, 2365
11 Ungar, G. and Organ, S. J. *J. Polym. Sci. Polym. Phys. Edn* 1990, **28**, 2353
12 Cheng, S. Z. D. and Chen, J. *J. Polym. Sci. Polym. Phys. Edn* 1991, **29**, 311
13 Kovacs, A. J., Gonthier, A. and Straupe, C. *J. Polym. Sci. Polym. Symp. Edn* 1975, **50**, 283
14 Kovacs, A. J., Straupe, C. and Gonthier, A. *J. Polym. Sci. Polym. Symp. Edn* 1977, **59**, 31
15 Lee, K. S. and Wegner, G. *Makromol. Chem. Rapid Commun.* 1985, **6**, 203
16 Alamo, R. G., Mandelkern, L., Stack, G. M., Krohnke, C. and Wegner, G. *Macromolecules* 1994, **27**, 147
17 Kovacs, A. J. and Gonthier, A. *Kolloid Z. Z. Polym.* 1972, **250**, 530
18 Sadler, D. M. and Gilmer, G. H. *Polym. Commun.* 1987, **28**, 242
19 Higgs, P. G. and Ungar, G. *J. Chem. Phys.* 1994, **100**, 640
20 Hoffman, J. D. *Polymer* 1992, **32**, 2828
21 Ungar, G. in 'Polymer Crystallization' (Ed. M. Dosiere), NATO ASI Series, Kluwer, Dordrecht, 1993, p. 63
22 Sadler, D. M. *J. Polym. Sci. Polym. Phys. Edn* 1985, **23**, 1533
23 Data obtained by Ross, G. S. and Ross, L. F., quoted in Hoffman, J. D. *Macromolecules* 1985, **18**, 786
24 Leung, W. M., Manley, R. St.John and Panaras, A. R. *Macromolecules* 1985, **18**, 760
25 Point, J. J. and Kovacs, A. J. *Macromolecules* 1980, **13**, 399
26 Hoffman, J. D. *Macromolecules* 1985, **18**, 786
27 Sadler, D. M. and Gilmer, G. H. *Phys. Rev. B* 1988, **38**, 5684
28 Sadler, D. M. *Nature (London)* 1987, **326**, 174
29 Organ, S. J. and Keller, A. *J. Mater. Sci.* 1985, **20**, 1571
30 Toda, A. *Polymer* 1991, **32**, 771
31 Hikosaka, M. and Seto, T. *Jpn J. Appl. Phys.* 1982, **21**, L332
32 Bassett, D. C., Olley, R. H. and Al Raheil, I. A. M. *Polymer* 1988, **29**, 1539
33 Mansfield, M. L. *Polymer* 1988, **29**, 1755
34 Point J. J. and Villers, D. *J. Cryst. Growth* 1991, **114**, 228
35 Point, J. J. and Villers, D. *Polymer* 1992, **33**, 2263
36 Sadler, D. M. *Polymer* 1983, **24**, 1401